AB-Note-2008-022 MD

SPS

Longitudinal impedance monitoring in the SPS with single short bunches at 26 GeV/c (RF on)

03 April 2008

abmdnote˙2008-022.tex

T. Bohl, T. Linnecar, E. Shaposhnikova

Date
1999-10-27
1999-11-17
2001-08-07
2003-09-04
2006-10-27
2006-11-17
2007-07-20
2007-11-01

Keywords: longitudinal, impedance

Summary

In the course of monitoring the low frequency impedance of the SPS over the years usually the quadrupole frequency shift as a function of intensity is measured with single bunches at 26 GeV/c with RF on using the peak detected signal. The additional acquisition of longitudinal bunch profiles allows the evaluation of various parameters of the injected beam, details of its quadrupole oscillation and the evolution of the bunch length as a function of time. Data acquired between 1999 and 2007 will be analysed in this respect. It will be shown that the bunch length data at 600 ms indicates clearly the effect of the SPS impedance reduction programme realised in 2000/2001 and that from then on the absolute value of the quadrupole frequency shift shows a tendency to increase over the years, indicating an impedance increase. However, it does not allow to monitor unambiguously the changes from one year to the next. The reason that the quadrupole frequency shift is not very well determined is attributed to the lack of reproducibility of bunch length and emittance at injection. In the future more attention will have to be paid to make these parameters reproducible.

1 Introduction

This Note summarises data acquired from 1999 to 2007 in the context of monitoring the longitudinal low-frequency impedance of the SPS using single short bunches at 26 GeV/c and by measuring the quadrupole frequency shift as a function of intensity [1]-[9]. The measurement series started in 1999 [1] in view of the SPS impedance reduction campaign [4] and were then repeated as often as an impedance change was expected.

The results of the measurements for 2007 [8] triggered a re-evaluation of the bunch profile data acquired from 1999 to 2007 with identical analysis methods which allow a consistent comparison of the beam parameters at injection and other data obtained from bunch profiles.

There are several ways to measure the quadrupole frequency, f_{2s}, at injection (see App. A). Initially longitudinal bunch profiles were only acquired to monitor the bunch length of the injected beam, as it is a parameter which should be kept constant to make meaningful quadrupole frequency shift measurements [6]. Later they were also used to determine f_{2s} and additional beam parameters.

The data will be treated in the same sequence as they were acquired and then summary plots will be shown which should facilitate their comparison.

2 Measurements

Typically the parameters of the injected bunch were as follows: BCT intensity, N_p in the range of $1 \times 10^{10} \leq N_p \leq 10 \times 10^{10}$, longitudinal emittance ("Mtchd Area", see [10]) measured in the PS with the tomoscope before bunch rotation between 0.1 eVs and 0.25 eVs, and the FWHM bunch length, τ_i, obtained in the SPS from the raw pick-up data[1] in the range of 0.9 ns $\leq \tau_i \leq$ 2.9 ns. For consistent measurements both the bunch length and the longitudinal emittance of the injected beam should not vary as a function of intensity.

An overview over all machine development sessions (MDs) at 26 GeV/c with single short bunches and RF on is provided in Sect. B, Table 1.

2.1 Data obtained with one acquisition

Each acquisition consists of longitudinal bunch profiles acquired at injection and 600 ms after injection. The latter measurement time was chosen in 1999 to observe a longitudinal emittance blow-up due to the microwave instability. This acquisition time was kept constant for all subsequent years. For each acquisition the intensity of the injected bunch is recorded. Throughout an MD the intensity of the injected beam, N_p, is varied.

For each acquisition the data will be analysed in view of obtaining information about (i) the bunch length at injection, (ii) the quadrupole oscillation amplitude, (iii) the quadrupole oscillation frequency, and (iv) the bunch length at 600 ms.

All bunch profiles were acquired with the wall current monitor AEW317.31 [11] and a digital oscilloscope with a -3 dB bandwidth of 1 GHz until 2003 and of 2.5 GHz in the following years.

The bunch length at injection, τ_i, is obtained from an acquisition of the first turn. For the purpose of this Note the FWHM bunch length of the raw pick-up data is fully adequate.

The relative quadrupole oscillation amplitude at injection is determined as $r_\tau = (\tau_{\max} - \tau_{\min})/(\tau_{\max} + \tau_{\min}) \times 2$, where $\tau_{\max}$ and $\tau_{\min}$ are the maximum and minimum FWHM bunch length of the raw bunch profiles acquired in the time interval $[0, t_{\rm obs}]$, with the observation time 5 ms$\leq t_{\rm obs} \leq$ 115 ms according to the MD.

The quadrupole oscillation frequency at injection is obtained from the bunch peak amplitude as a function of time during the same time interval as the quadrupole oscillation amplitude at injection. The bunch peak amplitude, $a_{\rm pk}$, is obtained either from the maximum amplitude of the raw bunch profile data or from the amplitude of a Gaussian fit of the fully corrected bunch profile data. In the following no distinction will be made between the two as it is irrelevant for the purpose of this Note.

The bunch length at 600 ms after injection is given by $\tau_f = (\tau_{\max} + \tau_{\min})/2$, where $\tau_{\max}$ and $\tau_{\min}$ are the maximum and minimum FWHM bunch length of the raw bunch profiles acquired in the time interval $[600\ {\rm ms}, 600\ {\rm ms} + t_{\rm obs}]$, where the observation time, $t_{\rm obs}$, is between 5 ms and 115 ms and which might vary from MD to MD.

2.2 Beam parameter variation as function of intensity

The next step of analysis concerns the variation of the previously mentioned parameters as a function of intensity of the injected beam.

[1]The FWHM bunch length of the raw pick-up data of the AEW pick-up can be converted to an approximate 4σ bunch length (corrected for pick-up and cable transfer function) by multiplying it with a factor of 1.4.

For all MDs the following analyses were made:

(1) a_{pk} data of the first turn were plotted against N_p. Under normal conditions the data are lying on a straight line. Data lying far off could always be identified as wrong measurements (attributed intensity was wrong, problem in injector, or other reasons). In this sense, all data presented here was lying on a straight line.

(2) τ_i versus N_p, to check the bunch length variation of the injected beam.

(3) $\tau_{\max}$, $\tau_{\min}$ and r_τ versus N_p. The variation of the quadrupole oscillation amplitude as a function of N_p indicates a variation of the longitudinal emittance of the injected beam for low intensities and shows the potential well distortion for higher intensities, provided the longitudinal emittance of the injected beam does not vary too much.

(4) quadrupole oscillation frequency as a function of intensity, N_p. It is described with a linear equation as $f_{2s} = f_{2s,0} + mN_p$.

In the following the quality of the acquired data is assessed for each MD and the relevant data are selected for further analysis which will take place in Sect. 3.

2.3 1999

In 1999 there were two MDs, one on 1999-11-15 (Measurement No. 1) and one on 1999-11-25 (Measurement No. 2). Bunch profile data were acquired to monitor τ_i and to determine τ_f. At this time it was not intended to measure the quadrupole frequency shift using the bunch profile data. Therefore the observation time at injection was fairly short, $t_{\mathrm{obs}} = 5.4$ ms.

For Measurement No. 1 τ_i as function of N_p, is practically constant, Fig. 1. However, Fig. 1 shows a large scatter of τ_i. From the data of Fig. 2 (left), $\tau_{\min}$ and $\tau_{\max}$ at injection versus N_p, the relative quadrupole oscillation amplitude was determined as a function of N_p, see Fig. 2 (right). This Figure shows the effect of the potential well distortion.

For Measurement No. 2 the variation of τ_i as function of N_p, Fig. 3, shows that there is a weak dependency of τ_i on N_p. It is visible because of the very small scatter of the τ_i.

From $\tau_{\min}$ and $\tau_{\max}$ at injection, see Fig. 4 (left), r_τ was determined, see Fig. 4 (right). This Figure shows that the longitudinal emittance of the injected beam is approximately the same as for Measurement No. 1.

Within the context of all MDs, Fig. 26 shows the mean value of τ_i, $\langle\tau_i\rangle$, its standard deviation and the range[2] of the τ_i for the Measurements No. 1 and No. 2. The distribution of the τ_i, Fig. 27, shows that for Measurement No. 2 the bunch length scatter is very small.

2.4 2001

The data of the year 2001 (acquired 2001-08-07) are the first one after the execution of the impedance reduction programme.

The data can be split in two parts (Measurement No. 3 and Measurement No. 4) according to the bunch length at injection, τ_i. Fig. 5 shows τ_i as a function of N_p. There is only a slight dependency of τ_i as a function of N_p. For Measurement No. 3, $\langle\tau_i\rangle = 2.0$ ns and for Measurement No. 4, $\langle\tau_i\rangle = 1.6$ ns. From $\tau_{\min}$ and $\tau_{\max}$ at injection, see Fig. 6, r_τ was determined, see Fig. 7. This Figure shows that the longitudinal emittance for Measurements No. 3 to No. 4 was not the same. As r_τ is constant as a function of N_p, the effect of the potential well distortion is very small in comparison to 1999 (see Fig. 2 and Fig. 7).

Fig. 26 shows $\langle\tau_i\rangle$, its standard deviation and the range of the τ_i for the Measurements No. 3 and No. 4 in comparison with previous measurements.

[2] in statistics the difference between the lowest and highest value of a distribution

The distributions of the τ_i for Measurements No. 3 and No. 4 are shown in Fig. 27. Fig. 28 displays r_τ versus N_p with respect to the other MDs.

The quadrupole oscillation frequency at injection versus N_p is shown in Fig. 8. As expected from the difference in $\langle\tau_i\rangle$, the slope, m, is different for the two measurements, namely (-1.6 ± 0.1) Hz$/10^{10}$ and (-1.3 ± 0.1) Hz$/10^{10}$, respectively.

2.5 2003

For Measurement No. 5 (2003-09-04) a strong variation of τ_i as a function of N_p is observed, Fig. 9. From $\tau_{\min}$ and $\tau_{\max}$ at injection, see Fig. 10 (left), r_τ was determined, see Fig. 10 (right). These Figures show that there is not only a large variation of τ_i versus N_p but also of $\tau_{\min}$, $\tau_{\max}$ and r_τ.

Fig. 26 shows $\langle\tau_i\rangle$, its standard deviation and the range of the τ_i for Measurement No. 5 in comparison with previous measurements. The distribution of the τ_i is the widest of all measurements, see Fig. 27. Fig. 28 displays r_τ versus N_p with respect to the other MDs.

The consequences of the bunch length variation show up when determining m. In Fig. 11 (top, left) you notice a strong variation of f_{2s} versus intensity. Therefore m was determined for several bunch intensity selections as shown in Table 1.

Meas.	Intensity Selection	τ_i[ns]	m/(Hz$/10^{10}$)
(i)	all values	0.9 - 2.4	-2.9 ± 0.1
(ii)	$N_p \leq 2 \times 10^{10}$	0.9 - 2.0	-7.1 ± 0.9
(iii)	$2 \times 10^{10} < N_p$	1.8 - 2.4	-2.2 ± 0.1
(iv)	$2 \times 10^{10} \leq N_p \leq 10 \times 10^{10}$	1.8 - 2.4	-2.5 ± 0.1

Table 1: Quadrupole frequency shift parameters for four bunch intensity selections. As τ_i increases monotonically with N_p this corresponds to a selection in bunch length, τ_i.

For comparison with previously obtained data, it made sense to calculate m from data in the intensity range $2 \times 10^{10} \leq N_p \leq 10 \times 10^{10}$ leading to $m = (-2.5 \pm 0.1)$ Hz$/10^{10}$. This corresponds to a significant increase of the absolute value of m with respect to 2001.

2.6 2006

There are three measurements available for 2006, Measurements No. 6 and No. 7, dated 2006-10-27, and No. 8, dated 2006-11-17.

2.6.1 2006-10-27

The acquisitions of 2006-10-27 have to be split in two parts according to τ_i, Measurements No. 6 and No. 7. Fig. 12 shows τ_i as a function of N_p for the two data sets. During the MD it was quickly realised that τ_i was too large for comparison with previous measurements, Fig. 12 (left). The parameters of the injected beam were modified to obtain shorter bunches, Fig. 12 (right). In both cases the bunch length varies considerably as a function of N_p. From $\tau_{\min}$ and $\tau_{\max}$ at injection, see Fig. 13 (left), r_τ was determined, see Fig. 13 (right). These Figures show that there is practically no variation of r_τ for Measurement No. 6 and a nearly factor 4 variation of r_τ for Measurement No. 7.

For comparison with previous measurements, Fig. 26 shows $\langle\tau_i\rangle$, its standard deviation and the range of τ_i for Measurements No. 6 and No. 7. For Measurement No. 6 the distribution of τ_i is fairly narrow as there are only a few acquisitions, see Fig. 27. For Measurement No. 7 it is very wide. This

has some consequences for the determination of the quadrupole frequency shift. Fig. 28 displays r_τ versus N_p with respect to the other MDs and confirms that the r_τ variation is the largest.

The variation of τ_i complicated determining the quadrupole frequency shift. There were several approaches to obtain m: (i) using all data, (ii) selecting data for $1.6\,\mathrm{ns} \leq \tau_i \leq 2.2\,\mathrm{ns}$, (iii) using only data of the first data set ($2.4\,\mathrm{ns} \leq \tau_i$), and finally (iv) using only the second data set ($\tau_i < 2.4\,\mathrm{ns}$). The results are shown in Fig. 15 and summarised in the Table 2.

Meas.	τ_i[ns]	m/(Hz/10^{10})
(i)	1.3 - 2.7	-3.0 ± 0.2
(ii)	1.6 - 2.2	-2.7 ± 0.6
(iii)	2.4 - 2.7	-3.0 ± 0.5
(iv)	1.3 - 2.4	-3.6 ± 0.4

Table 2: Quadrupole frequency shift parameters for the four bunch length selections.

For comparison with the other MDs the slope m obtained with the bunch length selection (iv) seems the most reasonable.

2.6.2 2006-11-17

For Measurement No. 8, dated 2006-11-17, the bunch length at injection is shown in Fig. 16. It is fairly independent of N_p. From $\tau_{\min}$ and $\tau_{\max}$ at injection, see Fig. 17 (left), r_τ was determined, see Fig. 17 (right). These Figures show that there is practically no variation of r_τ for Measurement No. 8.

Fig. 26 shows $\langle\tau_i\rangle$, its standard deviation and the range of the τ_i for Measurement No. 8 in comparison with previous measurements. For Measurement No. 8 the distribution of the τ_i is reasonable, see Fig. 27. Fig. 28 displays r_τ versus N_p with respect to the other MDs.

In the case of Measurement No. 8 it was difficult to obtain the quadrupole oscillation frequency because in a certain number of cases the oscillation was strongly damped. Without going into all details the values for m were found to be between (-2.5 ± 0.5) Hz/10^{10} and (-2.9 ± 0.5) Hz/10^{10}. Using the data where the quadrupole oscillation was well defined and not too quickly damped, $m = (-2.7 \pm 0.4)$ Hz/10^{10} was found, see Fig. 18. One observes a large scatter of the measurements.

2.7 2007

There are five measurements available for 2007, Measurement No. 9, dated 2007-07-20, and No. 10 to No. 13, dated 2007-11-01.

2.7.1 2007-07-20

For Measurement No. 9, the bunch length at injection is shown in Fig. 19. Given the large spread, it is fairly independent of intensity. From $\tau_{\min}$ and $\tau_{\max}$ at injection, see Fig. 20 (left), r_τ was determined for Measurement No. 9, see Fig. 20 (right). These Figures show that there is a slight negative trend for r_τ corresponding to a 30% decrease as function of N_p.

The quadrupole frequency shift is shown in Fig. 21. Unfortunately the intensity of the injected beam was limited to $N_p \leq 7 \times 10^{10}$ which does not allow m to be determined with the desired precision. A fit of the available data leads to $m = (-4.2 \pm 0.1)$ Hz/10^{10}.

2.7.2 2007-11-01

The beams for the Measurements No. 10 to No. 13 were produced in the PS under four different conditions (Table 3). The single bunch was either produced with shaving on or off (controlling the longitudinal emittance by changing the RF voltage during the acceleration ramp after transition) and with one or two 80 MHz cavities in operation for bunch rotation (changing the length of the bunch at extraction).

The combined plot of bunch length at injection, Fig. 22, is fairly flat as a function of N_p. However, there is a slight negative trend for Measurements No. 10 and No. 11 (shaving off).

From the four cases of $\tau_{\min}$ and $\tau_{\max}$ at injection versus N_p, see Fig. 23, r_τ was determined, see Fig. 24. The slope of this curve is practically flat for Meas. No. 10 and No. 12 (2×80 MHz) and has a negative slope for No. 11 and No. 13 (1×80 MHz).

The quadrupole frequency shift for the four measurements is shown in Fig. 25 and summarised in Table 3.

Meas.	Conditions	$\langle\tau_i\rangle$[ns]	m/(Hz/10^{10})
10	2×80 MHz, shaving off	1.9	-2.2 ± 0.3
11	1×80 MHz, shaving off	2.6	-3.1 ± 0.1
12	2×80 MHz, shaving on	1.4	-3.4 ± 0.2
13	1×80 MHz, shaving on	2.0	-4.1 ± 0.1

Table 3: Measurement conditions, $\langle\tau_i\rangle$, τ_i, and m for the four measurements of 2007-11-01.

With respect to previous measurements, Measurement No. 11 should clearly not be considered further because of the large τ_i.

3 Comparison of the machine development results

The results of the MDs, namely bunch length at 600 ms (τ_f) and quadrupole frequency shift (m), are functions of the longitudinal emittance and bunch length of the injected beam and of the low-frequency machine impedance. To determine the evolution of the impedance over the years it is therefore desirable that neither the longitudinal emittance nor the bunch length of the injected beam vary as a function of N_p nor as a function of time (the years 1999 to 2007). In the following the acquired data will be reviewed with these points in mind.

3.1 Bunch length at injection and longitudinal emittance

Fig. 26 (top) shows the mean bunch length at injection, $\langle\tau_i\rangle$, and its standard deviation, whereas Fig. 26 (bottom) shows the range of the τ_i. For Measurements No. 6 and No. 11 one observes that $\langle\tau_i\rangle$ lies outside the main population and for the No. 5, No. 7 and No. 13 it is the bunch length range, which is very large. The corresponding bunch length distributions are shown in Fig. 27. This Figure shows that the large spread of Measurement No. 13 is due to a single measurement and can be ignored.

The variation of the relative quadrupole oscillation amplitude for small N_p, Fig. 28, as already said, is an indication of the variation of the longitudinal emittance of the injected bunch. It should be taken into account when comparing the results of various MDs.

3.2 Bunch length at 600 ms

The bunch length at 600 ms, τ_f, as a function of intensity for all measurements is shown in Fig. 29 together with τ_i. Measurement No. 2 is the most clean one (Meas. No. 1 and No. 2 were made before the impedance reduction campaign). The ratio of τ_f/τ_i versus intensity is shown in Fig. 30.

Taking all measurements and restricting τ_i to the same range of values as for Measurement No. 2 leads to Fig. 31. It summarises what can be said for the bunch length at 600 ms versus bunch intensity data. The difference between the bunch lengthening before the pumping port shielding effort (Meas. No. 1 and No. 2) and after this event (Meas. No. 3 to No. 13) is clearly visible. However the later change of the longitudinal SPS impedance is not visible in the bunch length data.

3.3 Quadrupole frequency shift

The quadrupole frequency shift data of all measurements are summarised in Table 4.

No.	Date	$\langle\tau_i\rangle$ [ns]	$r_{\tau,0}$	m/(Hz/10^{10})	$f_{2s,0}$ [Hz]	Remarks
1	1999-11-15	1.9	0.30 ± 0.10			$t_{\rm obs}$ too short
2	1999-11-25	1.6	0.35 ± 0.05			$t_{\rm obs}$ very short
3	2001-08-07_1	2.0	0.55 ± 0.10	-1.6 ± 0.1	308 ± 0.5	
4	2001-08-07_2	1.6	0.25 ± 0.10	-1.3 ± 0.1	308 ± 0.5	
5	2003-09-04	1.9	0.55 ± 0.10	-2.5 ± 0.1	324 ± 0.6	
6	2006-10-27_1	2.6	0.55 ± 0.05	-3.0 ± 0.2	310 ± 1.6	$\langle\tau_i\rangle$ outside range
7	2006-10-27_2	1.8	0.60 ± 0.30	-2.7 ± 0.6	307 ± 4.9	
	2006-10-27_3	2.6		-3.0 ± 0.6	311 ± 4.3	$\langle\tau_i\rangle$ outside range
	2006-10-27_4	1.8		-3.6 ± 0.6	313 ± 2.6	
8	2006-11-17	2.1	0.25 ± 0.10	-2.5 ± 0.5	309 ± 2.5	
9	2007-07-20	2.1	0.65 ± 0.10	-4.5 ± 0.1	310 ± 0.5	
10	2007-11-01_1	1.9	0.20 ± 0.05	-2.2 ± 0.3	298 ± 2.5	2×80 MHz, shaving off
11	2007-11-01_2	2.6	0.80 ± 0.05	-3.1 ± 0.1	302 ± 0.7	1×80 MHz, shaving off, $\langle\tau_i\rangle$ outside range
12	2007-11-01_3	1.4	0.30 ± 0.05	-3.4 ± 0.2	314 ± 1.1	2×80 MHz, shaving on
13	2007-11-01_4	2.0	0.80 ± 0.10	-4.1 ± 0.1	314 ± 0.8	1×80 MHz, shaving on

Table 4: Quadrupole frequency shift data m and $f_{2s,0}$. $r_{\tau,0}$ the relative amplitude of the quadrupole oscillation, $r_{\tau,0}$, for low N_p. The errors for m and $f_{2s,0}$ are shown as they were calculated by the fit routine (using Mathematica). The actual errors are certainly larger.

The data marked with "$\langle\tau_i\rangle$ outside range" are not further considered. The Table shows the considerable variation of $\langle\tau_i\rangle$. As we have seen here and in [6] the quadrupole frequency shift depends on τ_i. Therefore it makes sense to group the data according to $\langle\tau_i\rangle$.

The combined distribution of τ_i for the years 1999 to 2007 is shown in Fig. 32. This Figure suggests that a selection of 1.7 ns$\leq \tau_i \leq$2.3 ns and a re-evaluation of m with this selection should allow a comparison of the quadrupole frequency shift for 1999 to 2007.

With this selection all data from Measurement No. 3, 90% of the data from Measurement No. 5, 35% of the data from Measurement No. 7, 98% of the data from Measurement No. 8, 98% of the data from Measurement No. 9, 100% of the data from Measurement No. 10 and 97% of the data from Measurement No. 13 could be retained and re-evaluated where necessary, see Fig. 33. The results of these re-evaluations are summarised in Table 5.

Meas.	Date	$\langle\tau_i\rangle$ [ns]	$r_{\tau,0}$	m/(Hz/10^{10})	Remarks
3	2001-08-07_1	2.0	0.55 ± 0.10	-1.6 ± 0.1	
5	2003-09-04	1.9	0.55 ± 0.10	-2.5 ± 0.1	
7	2006-10-27_2	1.8	0.60 ± 0.30	-2.7 ± 0.6	
8	2006-11-17	2.1	0.25 ± 0.10	-2.5 ± 0.5	
9	2007-07-20	2.1	0.65 ± 0.10	-4.5 ± 0.1	
10	2007-11-01_1	1.9	0.20 ± 0.05	-2.2 ± 0.3	2×80 MHz, shaving off
13	2007-11-01_4	2.0	0.80 ± 0.10	-4.1 ± 0.1	1×80 MHz, shaving on

Table 5: Quadrupole frequency shift data m for 1.7 ns$\leq \tau_i \leq$2.3 ns.

Introducing $r_{\tau,0}$ as the value of r_τ for low intensities, it is possible to compare the longitudinal emittance of the injected beam for low intensities. If the bunch length stays approximately constant with increasing N_p, $r_{\tau,0}$ would also give an indication of the longitudinal emittance for higher intensities.

Fig. 27 shows that Measurements No. 10 and No. 13 have a very similar distribution of τ_i but their m is significantly different, $m = -2.2$ and -4.1, respectively. This seems to be a consequence of the different longitudinal emittance of the injected beam: $r_{\tau,0} = 0.2$ and 0.8, respectively.

Using $r_{\tau,0}$ as an indicator of the emittance of the injected beam, it is possible to make a further selection based on this parameter. As Table 5 shows, Measurements No. 8 and No. 10 have a particularly low $r_{\tau,0}$ and can therefore be eliminated to obtain a consistent data set for m with $0.55 \leq r_{\tau,0} \leq 0.80$.

The slope, m, of the quadrupole frequency shift for all valid measurements is shown in Fig. 34. One observes a negative going trend of m as a function of time.

4 Conclusions

The variation of bunch length and longitudinal emittance at injection was analysed for the MDs used to determine the evolution of the longitudinal low-frequency impedance since 1999. The bunch length data at 600 ms indicates clearly the effect of the impedance reduction programme. Since the SPS impedance reduction in 2000, the quadrupole frequency shift parameter m has a tendency to decrease over the years, i.e. the impedance is increasing, but it does not allow the changes from one year to the next to be monitored precisely.

The reason that the quadrupole frequency shift is not very well determined is attributed to the lack of reproducibility of bunch length and longitudinal emittance at injection. In the future more attention will have to be paid to make these parameters reproducible.

A next step in the interpretation of the presented MD data could be a comparison of the observed variation of the slope m with the one calculated from the expected impedance change and a comparison of the data presented here with the quadrupole frequency shift data obtained by other methods (as mentioned in App. A, see also [8], [9]).

5 Acknowledgements

A lot of persons were involved to produce the beam for the machine developments. We would like to thank the PS Booster, PS and SPS operators, and our PS and SPS RF Low Level colleagues H. Damerau, S. Hancock, M. Schokker, and U. Wehrle for their contributions.

A Measurements

During the MDs to monitor the SPS longitudinal impedance typically the following data are acquired. The longitudinal emittance of the injected beam is determined in the PS with the tomoscope using the "Mtchd Area"-emittance value [10]. The bunch length at injection is either obtained at extraction from the PS with the BSM [13] or from a wall current monitor in the SPS. The intensity of the injected beam is measured with the BCT shortly after injection and small losses at injection are therefore discarded.

The quadrupole oscillation frequency at injection is determined from the peak detected signal using the cursor function of a digital oscilloscope. The peak detected signal is low-pass filtered to reduce the revolution frequency component. The quadrupole oscillation frequency is also acquired with a low frequency spectrum analyser triggered a few 100 ms after injection (to get rid of transient input overload). When the bunch is unstable the spectrum is dominated by the coherent quadrupole frequency otherwise by the incoherent frequency distribution.

The use of the bunch profile data obtained from a wall current monitor is discussed in the main text. Typical bunch length and peak amplitude signals are shown in Fig. 35. Typical quadrupole oscillation data are shown in Fig. 36. In the strongly damped case the oscillation frequency changes as the amplitude of the oscillation is reducing.

B Machine developments with single short bunches and RF on

Table 1 gives an overview of all MDs with single short bunches and RF on at 26 GeV/c. Not all of the listed MDs were intended to determine the low frequency/inductive part of the machine impedance.

The RF voltage for all MDs was checked by comparing $f_{2s,0}$. For the MDs during the lead ion runs, where additional phase shifters are installed in the cavity return path, the error between requested and actual RF voltage is increased due to counterphasing errors and then an RF voltage check is especially recommended.

Date	τ [ns]	ϵ [eVs]	Remarks
1996-11-20			not discussed
1999-11-15			only a few frames at injection and at 600 ms; not enough data for τ_f; see [3], [5], [8]
1999-11-25			$t_{\rm obs}$ too short for determination of f_{2s} and m from bunch profile data; [1], [2], [3], [4], [5], [8]
2001-08-07	2.5 - 3.5	0.15 - 0.16	[3], [4], [5], [8]
2002-09-23	3.0	0.13	no measurement of f_{2s}
2003-09-04		0.13 - 0.19	[8]
2006-10-27			[7]
2006-11-17			[8]
2007-07-20	3.0-3.2	0.12 - 0.21	[8]
2007-11-01		0.10 - 0.23	[9]

Table 1: MDs with single short bunches on a 26 GeV/c flat bottom and RF on (900 kV). The beam parameters at extraction from the PS are the 4σ bunch length, τ, and the longitudinal emittance, ϵ, measured with the tomoscope in the PS before bunch rotation.

C Figures

C.1 1999

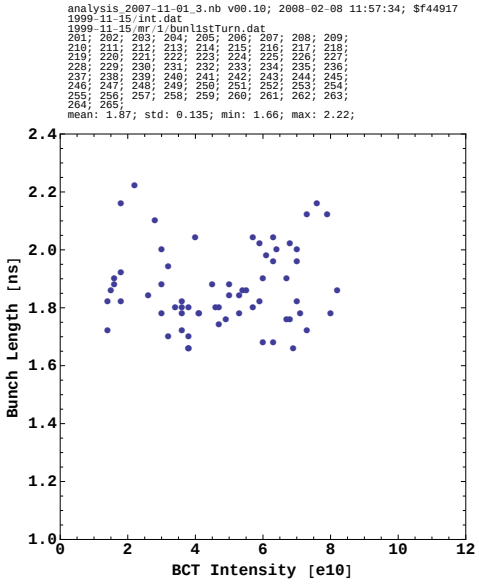

Figure 1: τ_i versus N_p for Measurement No. 1., 1999-11-15.

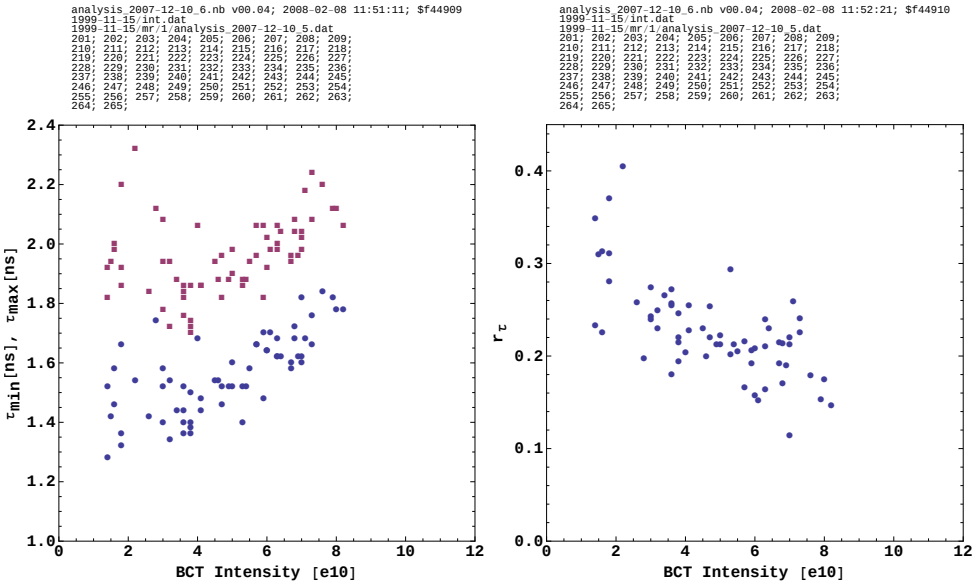

Figure 2: $\tau_{\min}$, $\tau_{\max}$ for $[0, t_{\text{obs}}]$ versus N_p (left) and r_τ versus N_p (right). Measurement No. 1, $t_{\text{obs}} = 5.4$ ms, 1999-11-15.

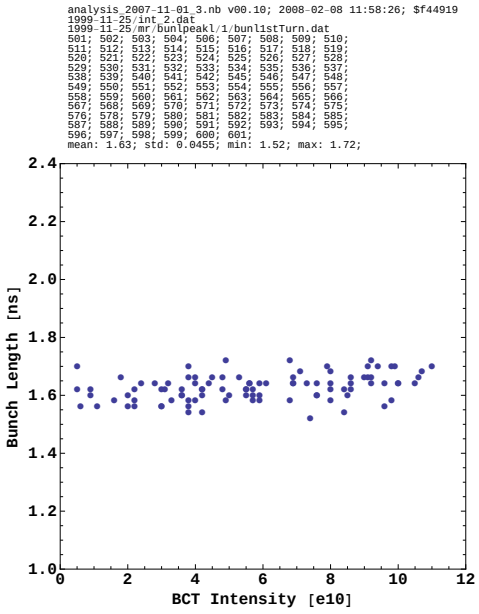

Figure 3: τ_i versus N_p for Measurement No. 2. 1999-11-25.

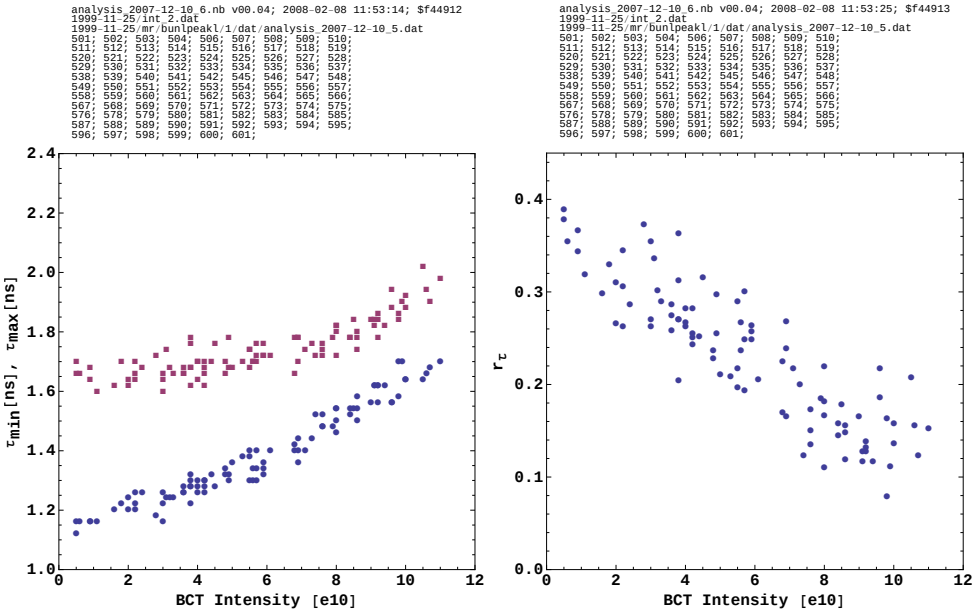

Figure 4: $\tau_{\min}$, $\tau_{\max}$ for $[0, t_{\text{obs}}]$ versus N_p (left) and r_τ versus N_p (right). Measurement No. 2, $t_{\text{obs}} = 5.6$ ms, 1999-11-25.

C.2 2001

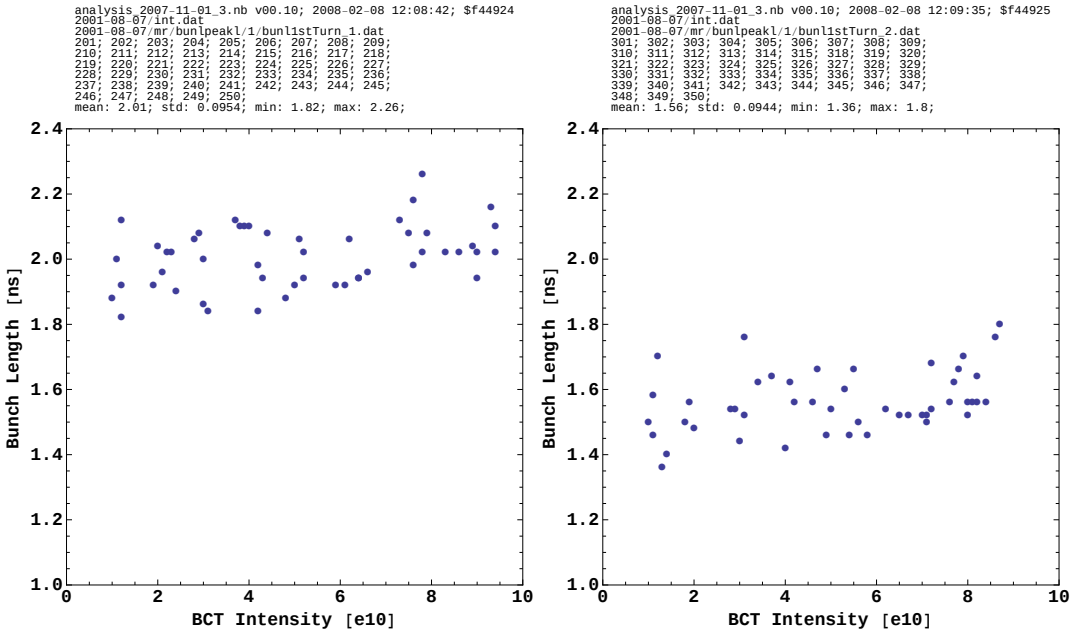

Figure 5: τ_i versus N_p for Measurement No. 3 (left), and for No. 4 (right). 2001-08-07.

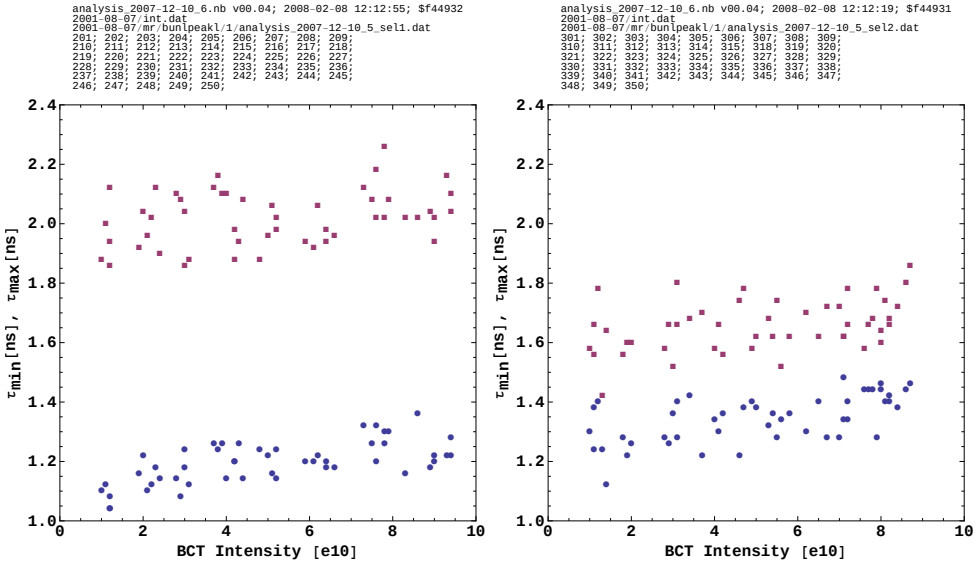

Figure 6: $\tau_{\min}$, $\tau_{\max}$ for $[0, t_{\text{obs}}]$ versus N_p for Measurement No. 3 (left), and for No. 4 (right), $t_{\text{obs}} = 20.6$ ms, 2001-08-07.

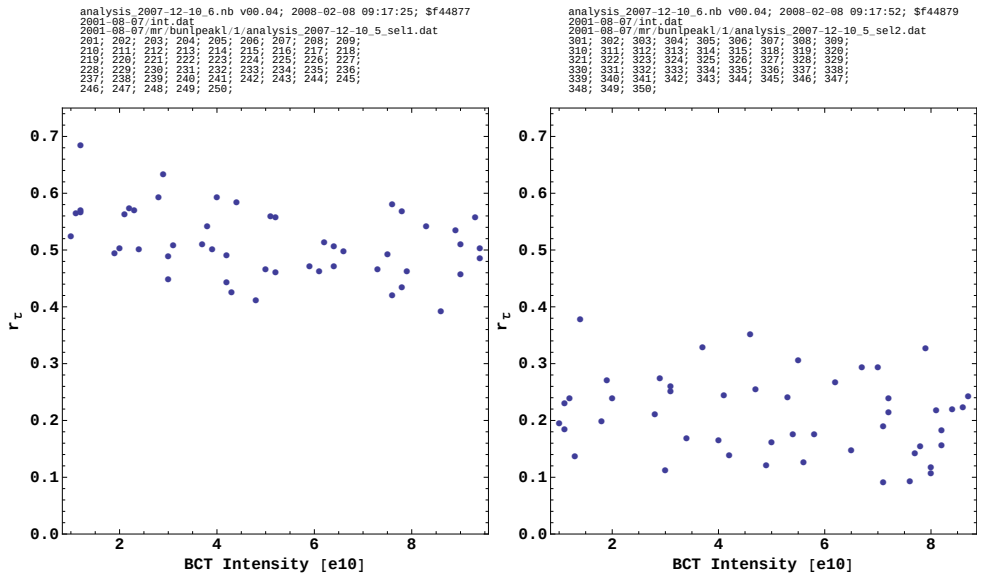

Figure 7: r_τ versus N_p for Measurement No. 3 (left), and for No. 4 (right). 2001-08-07.

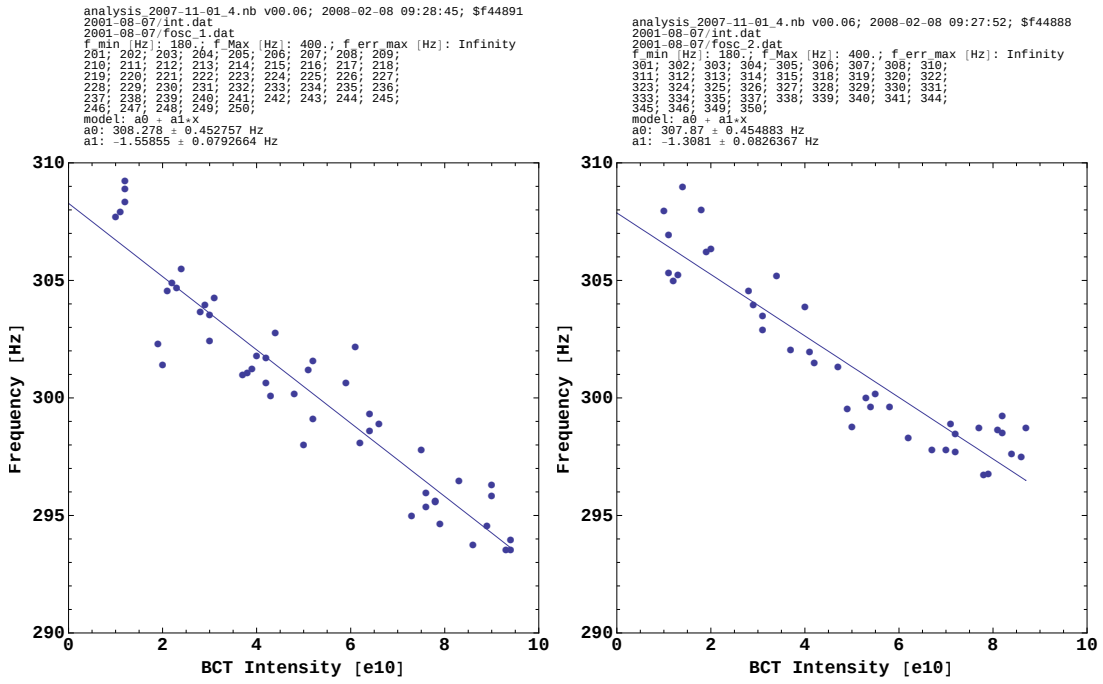

Figure 8: Quadrupole oscillation frequency at injection N_p for Measurement No. 3 (left), No. 4 (right). For the fit results see Table 4 (p. 7). 2001-08-07.

C.3 2003

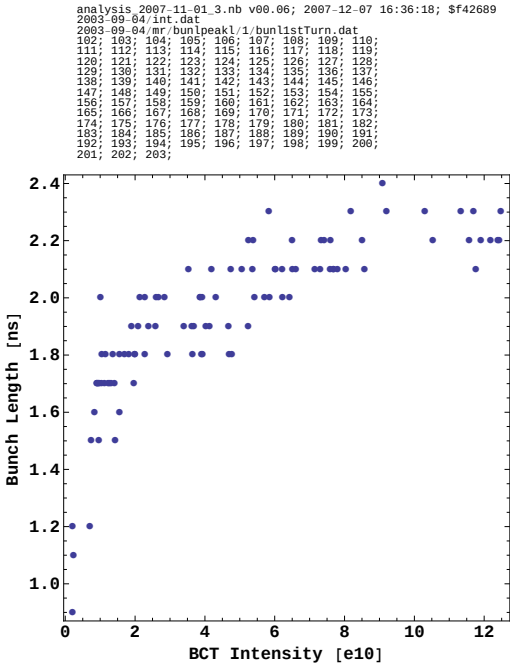

Figure 9: τ_i versus N_p. Measurement No. 5, 2003-09-04.

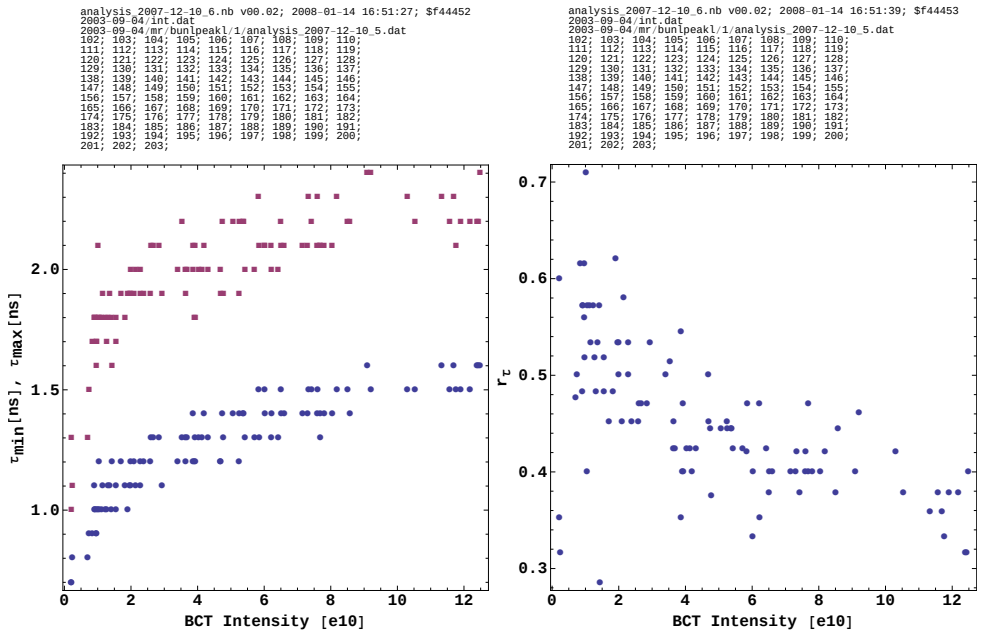

Figure 10: $\tau_{\min}$, $\tau_{\max}$ for $[0, t_{\text{obs}}]$ versus N_p (left) and r_τ versus N_p (right). Measurement No. 5, $t_{\text{obs}} = 16.8$ ms, 2003-09-04.

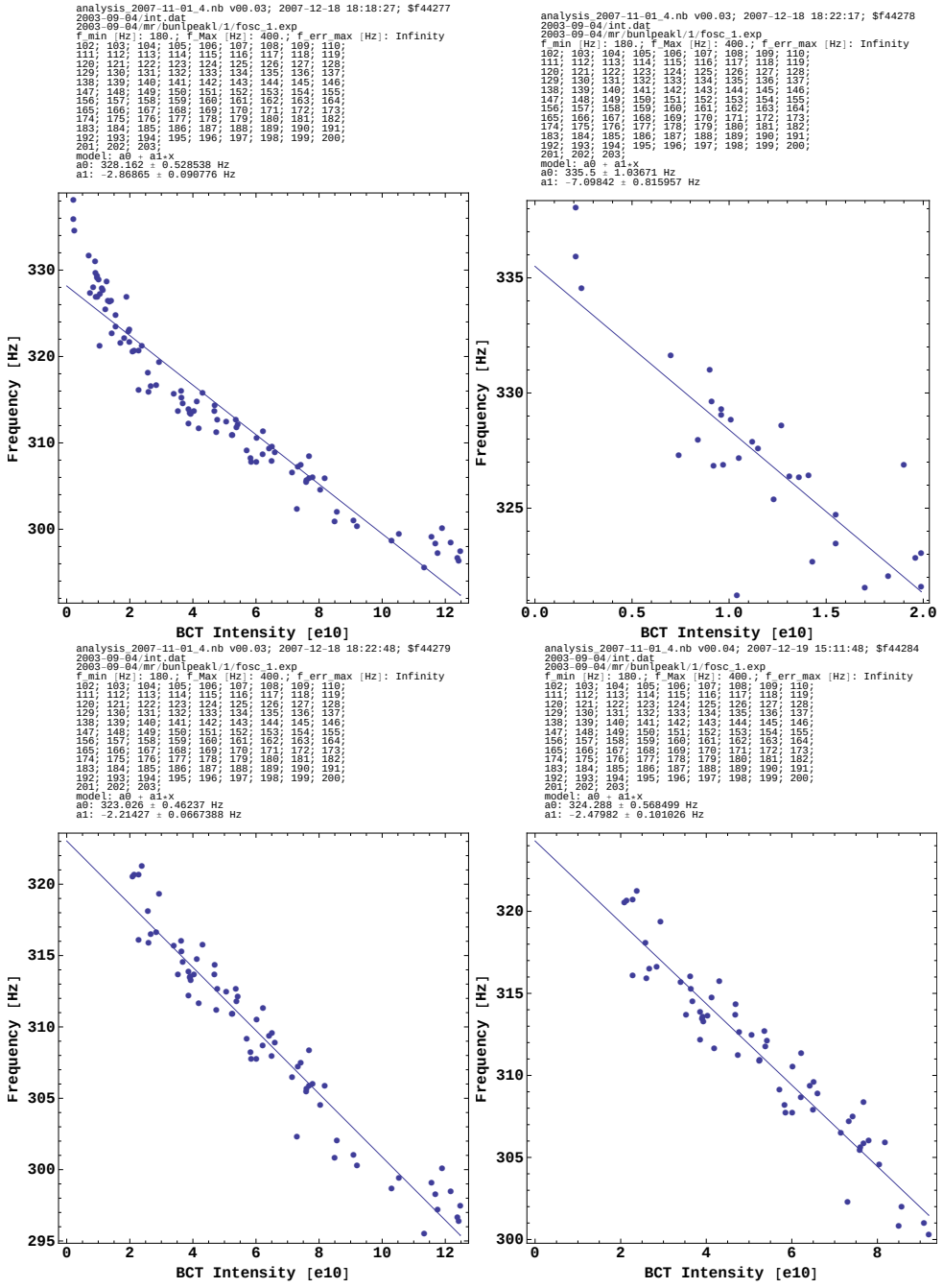

Figure 11: Quadrupole oscillation frequency at injection versus N_p for four intensity ranges: all intensities (top, left), $N_p < 2 \times 10^{10}$ (top, right), $2 \times 10^{10} < N_p$ (bottom, left) and $2 \times 10^{10} \leq N_p \leq 10 \times 10^{10}$. Measurement No. 5, 2003-09-04. For the fit results see Table 4 (p. 7).

C.4 2006

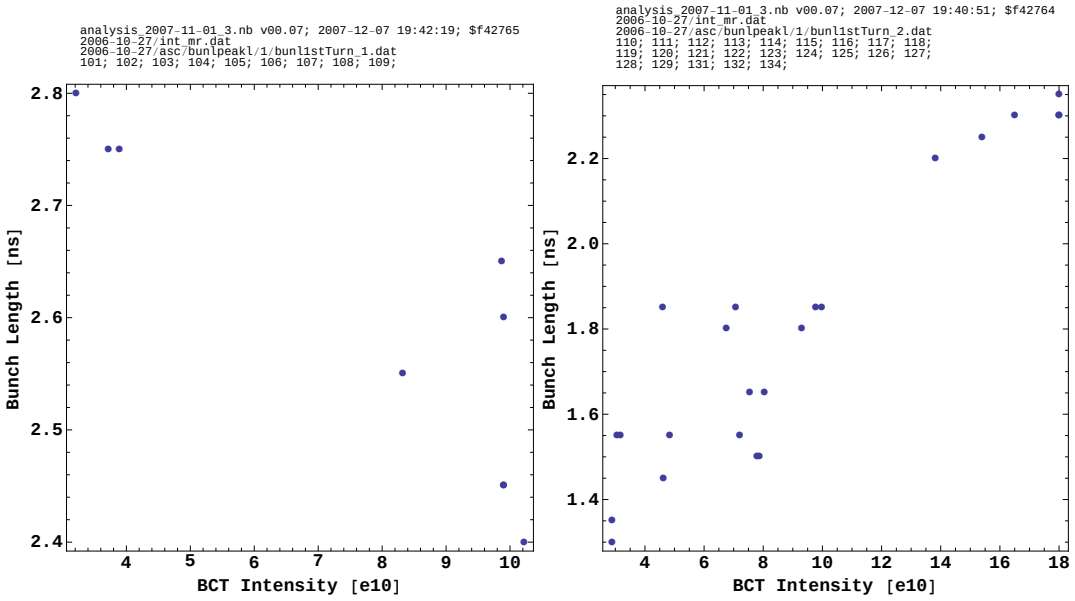

Figure 12: τ_i versus N_p for Measurement No. 6 (left) and No. 7 (right). 2006-10-27.

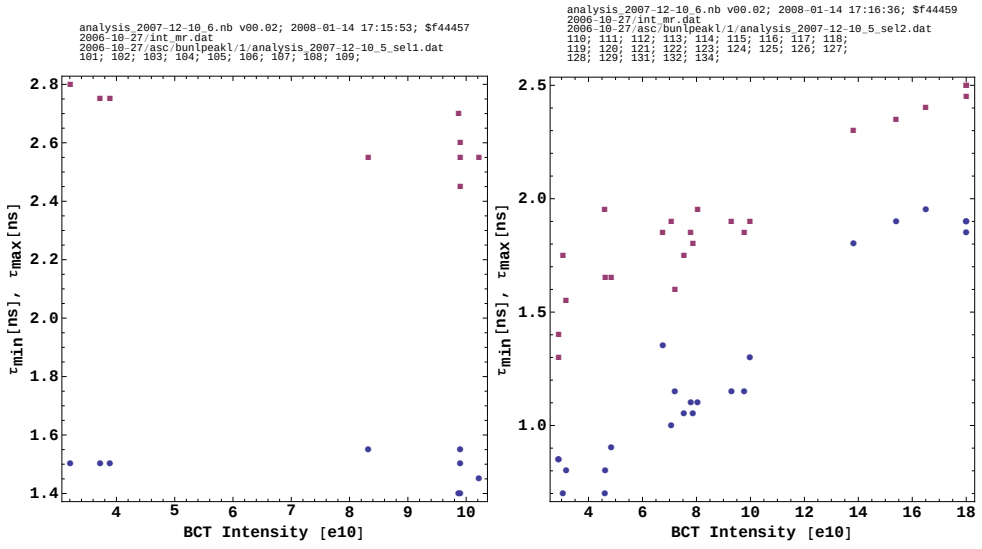

Figure 13: $\tau_{\min}$, $\tau_{\max}$ for $[0, t_{\text{obs}}]$ versus N_p. Measurement No. 6 (left) and No. 7 (right), $t_{\text{obs}} = 29.6$ ms, 2006-10-27.

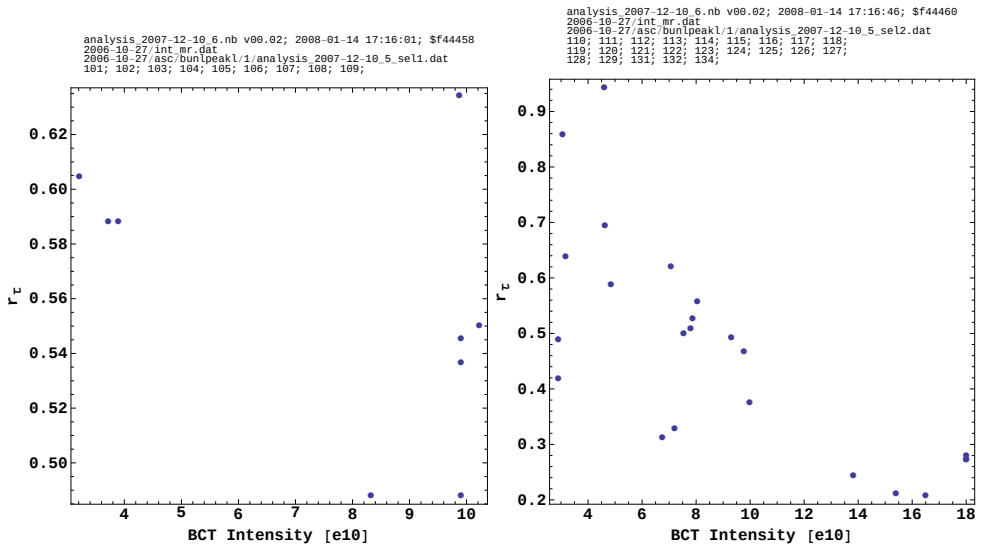

Figure 14: r_τ versus N_p. Measurement No. 6 (left) and No. 7 (right). 2006-10-27.

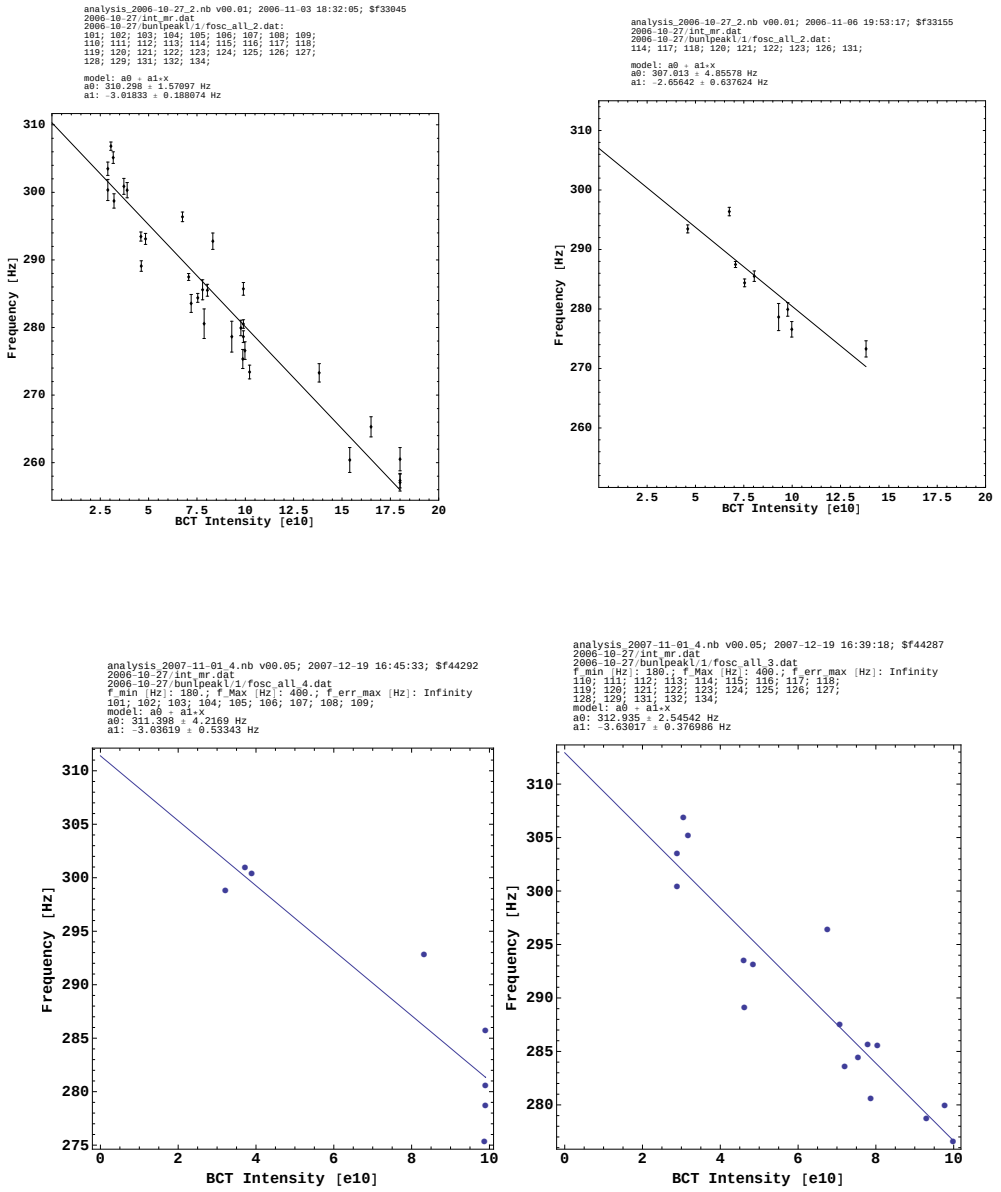

Figure 15: Quadrupole oscillation frequency at injection versus N_p for the four cases discussed in the text (see Table 2. Measurement No. 6 and No. 7, 2006-10-27. For the fit results see Table 4 (p. 7).

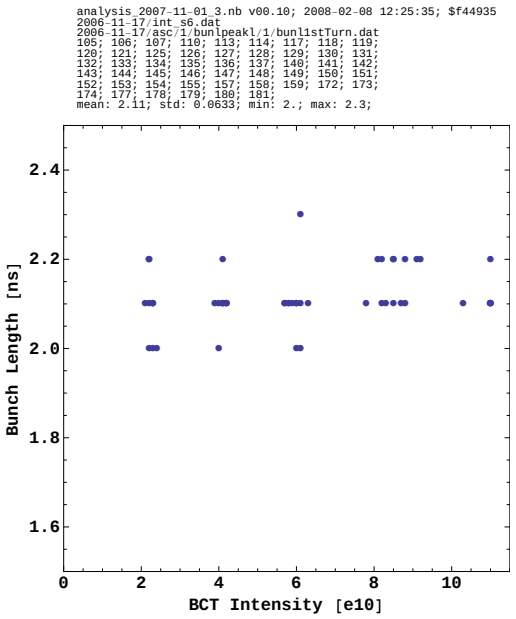

Figure 16: τ_i versus N_p. Measurement No. 8, 2006-11-17.

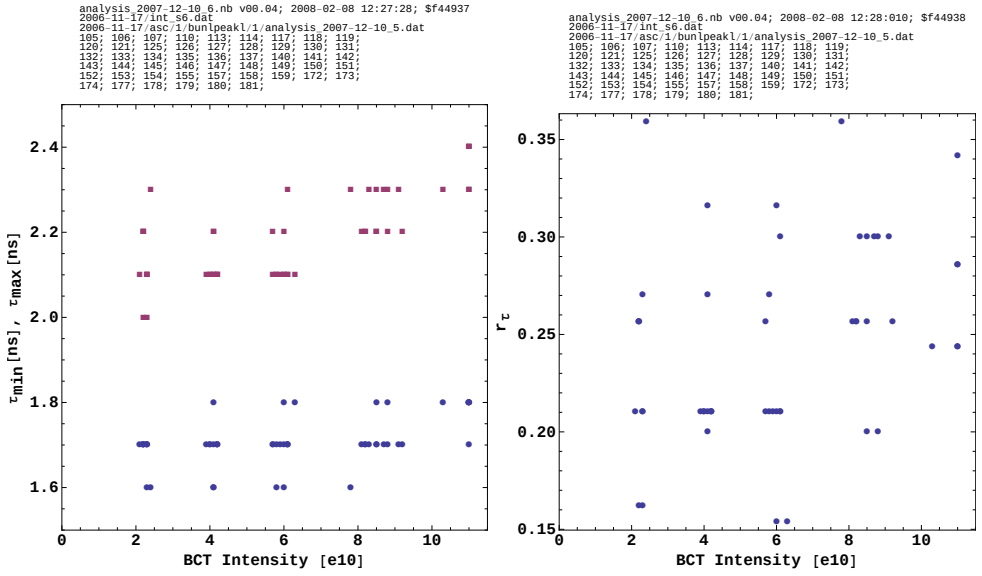

Figure 17: $\tau_{\min}$, $\tau_{\max}$ for $[0, t_{\text{obs}}]$ versus N_p (left) and r_τ versus N_p (right). Measurement No. 8, $t_{\text{obs}} = 74.5$ ms, 2006-11-17.

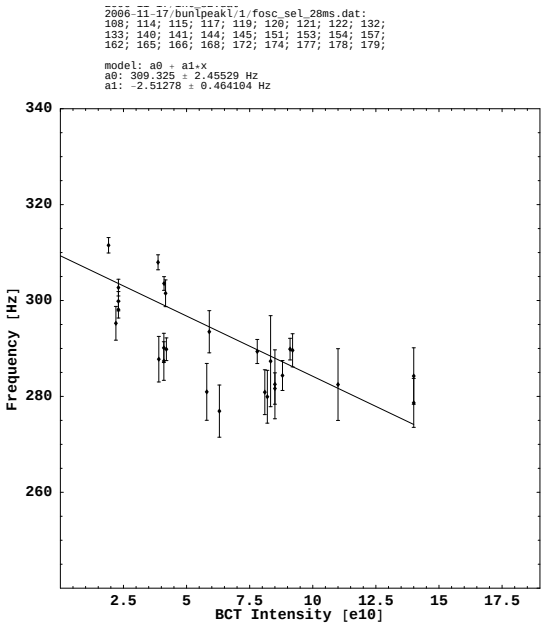

Figure 18: Quadrupole oscillation frequency at injection versus N_p. For the fit results see Table 4 (p. 7). Measurement No. 8, 2006-11-17.

C.5 2007

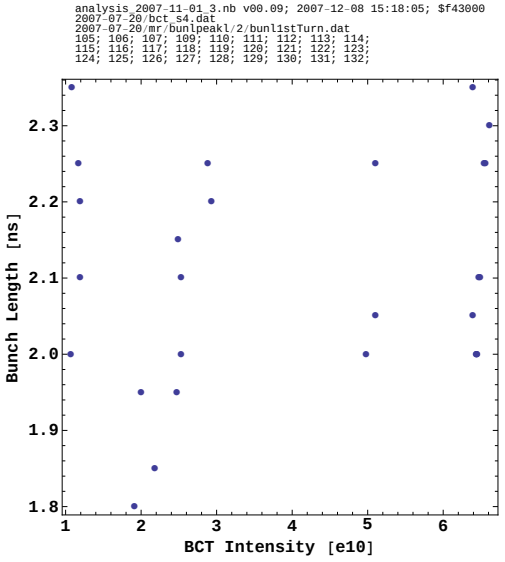

Figure 19: τ_i versus N_p. Measurement No. 9, 2007-07-20.

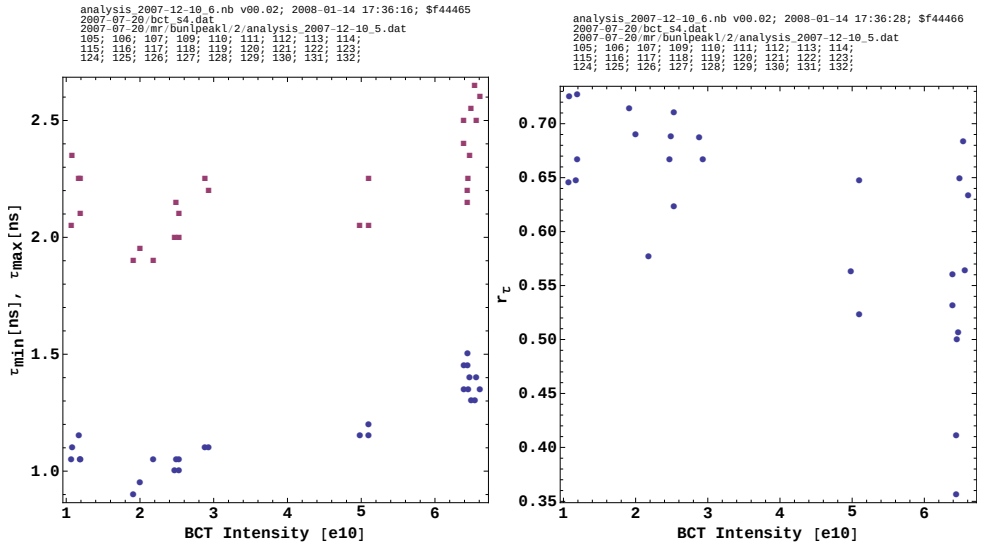

Figure 20: $\tau_{\min}$, $\tau_{\max}$ for $[0, t_{\text{obs}}]$ versus N_p (left) and r_τ versus N_p (right). Measurement No. 9, $t_{\text{obs}} = 114.9$ ms, 2007-07-20.

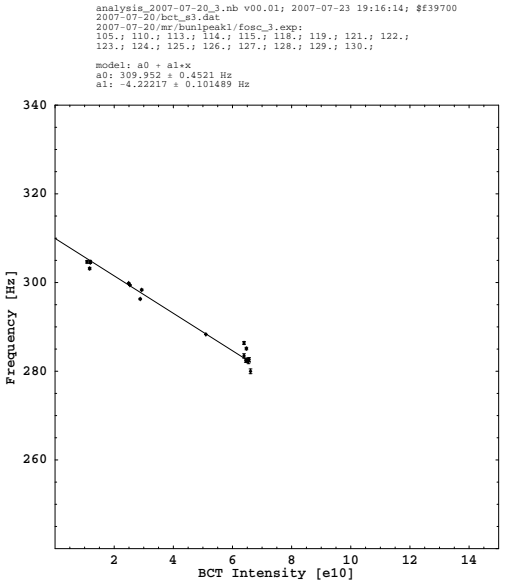

Figure 21: Quadrupole oscillation frequency at injection versus N_p. For the fit results see Table 4 (p. 7). 2007-07-20.

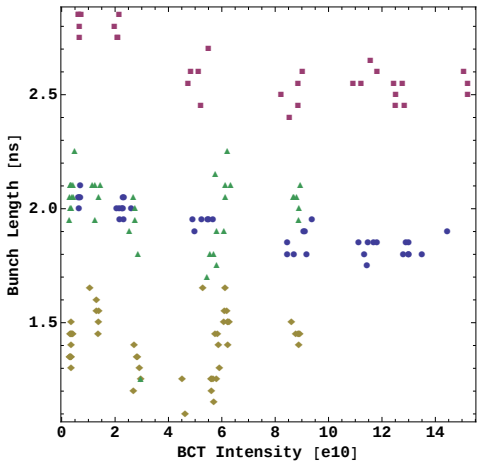

Figure 22: τ_i versus N_p. Measurement No. 10 (blue circle), No. 11 (red square), No. 12 (yellow diamond) and No. 13 (green triangle). 2007-11-01.

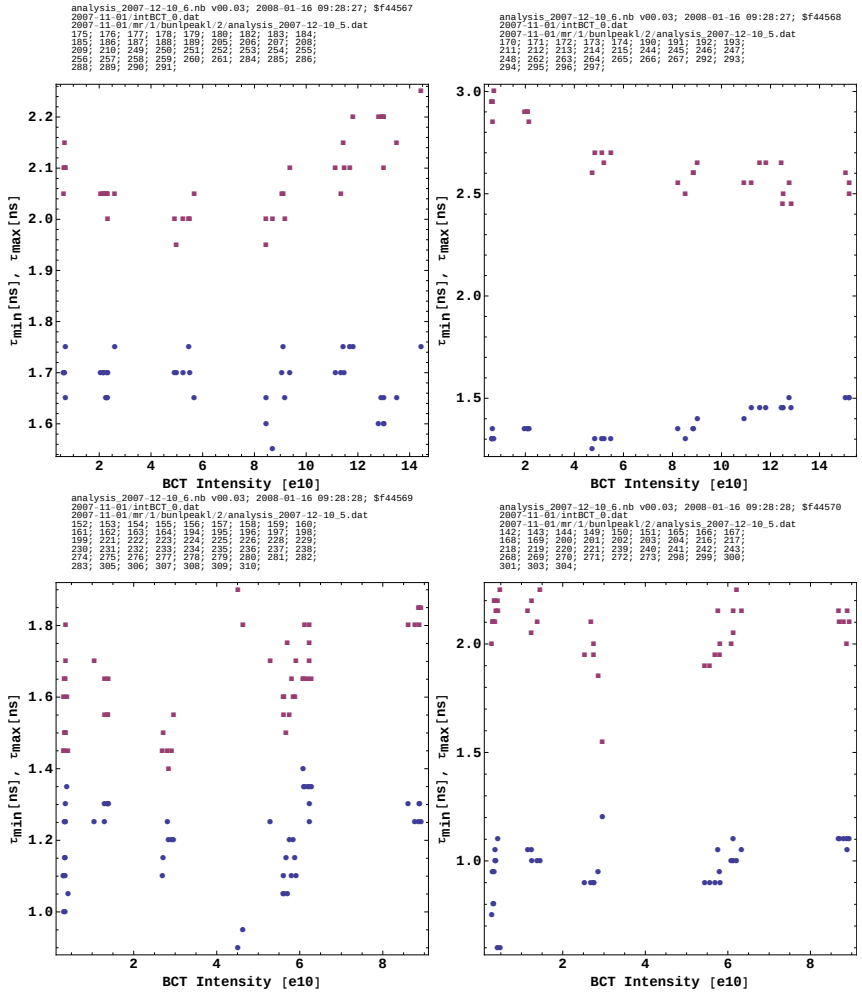

Figure 23: $\tau_{\min}$, $\tau_{\max}$ for $[0, t_{\text{obs}}]$ versus N_p. Meas. No. 10 (top left), Meas. No. 11 (top right), Meas. No. 12 (bottom left), Meas. No. 13 (bottom right), $t_{\text{obs}} = 57.4$ ms, 2007-11-01.

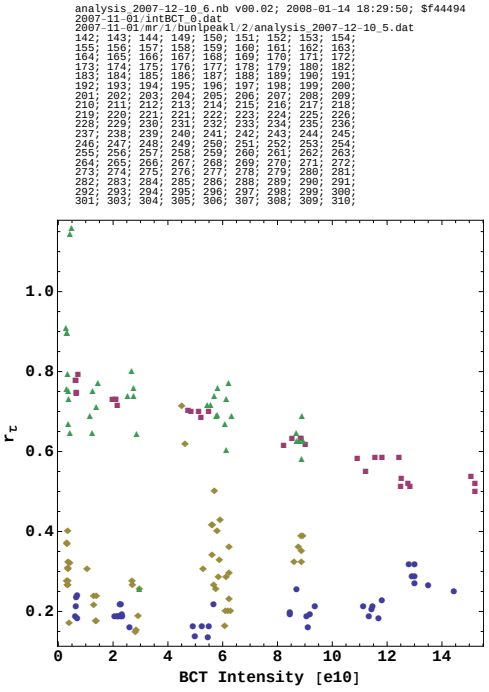

Figure 24: r_τ versus N_p. Measurement No. 10 (blue circle), No. 11 (red square), No. 12 (yellow diamond) and No. 13 (green triangle). $t_{\rm obs} = 57.4$ ms, 2007-11-01.

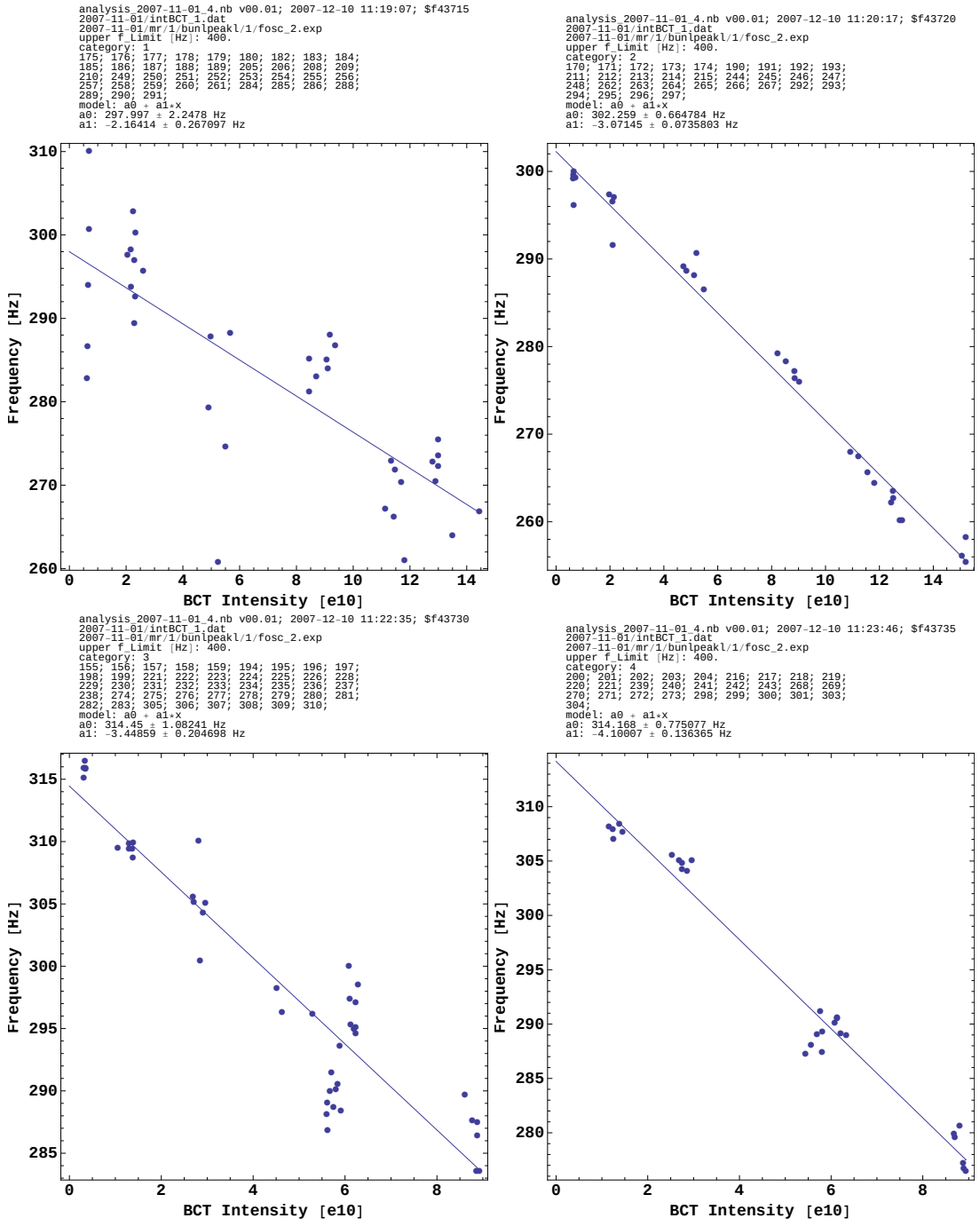

Figure 25: Quadrupole oscillation frequency at injection versus N_p. For the fit results see Table 4 (p. 7). Meas. No. 10 (top left), Meas. No. 11 (top right), Meas. No. 12 (bottom left), Meas. No. 13 (bottom right), 2007-11-01.

C.6 Overview plots

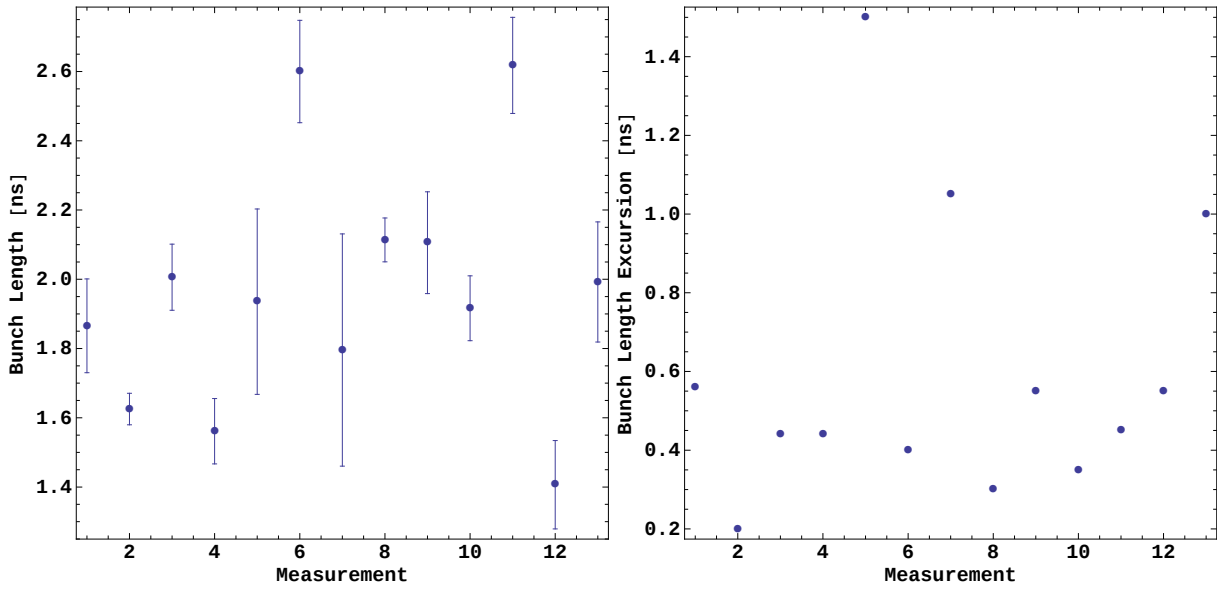

Figure 26: $\langle \tau_i \rangle$ and its standard deviation (left). Difference of maximum and minimum bunch τ_i (right) for all measurements.

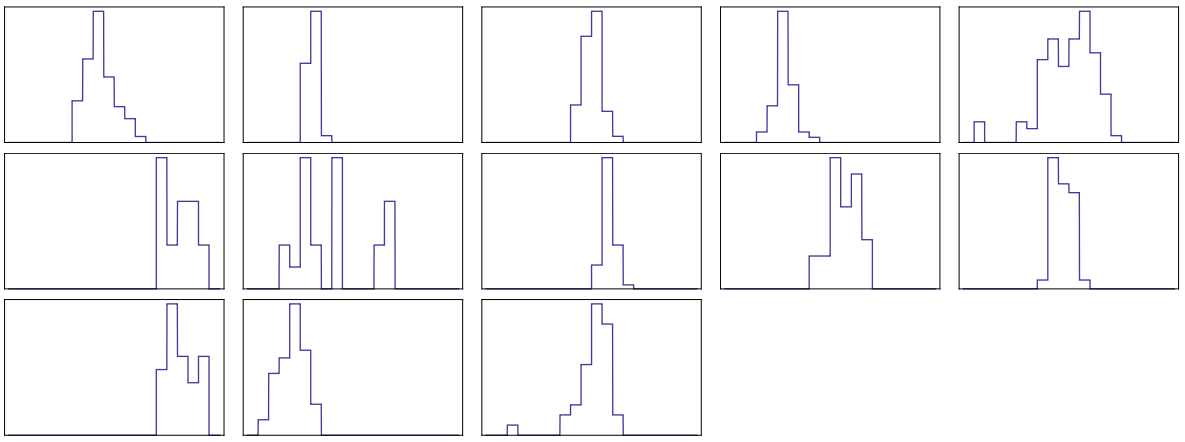

Figure 27: τ_i distribution for Measurement No. 1 (top left) to No. 13 (bottom right). Horiz. axis: 0.9 ns to 3.0 ns, vertical axis normalised for each measurement, bin width 0.1 ns.

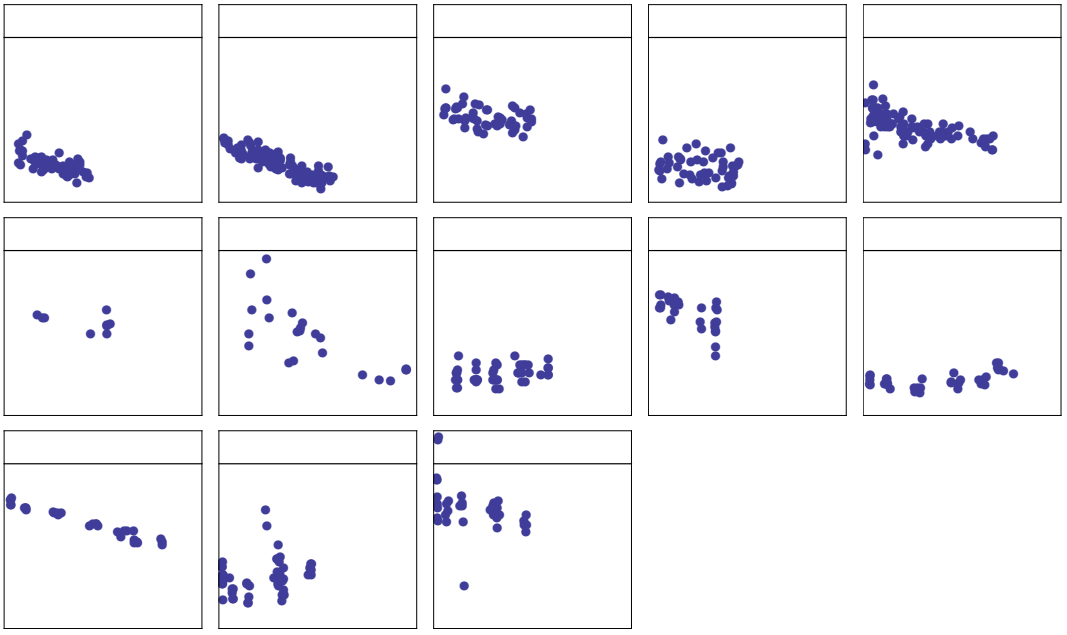

Figure 28: r_τ versus N_p for all measurements. Horiz. scale: $0 - 19 \times 10^{10}$, vert. scale: $0 - 1.2$, horizontal line indicating a ratio of 1. Measurement No. 1 (top left) to No. 13 (bottom right).

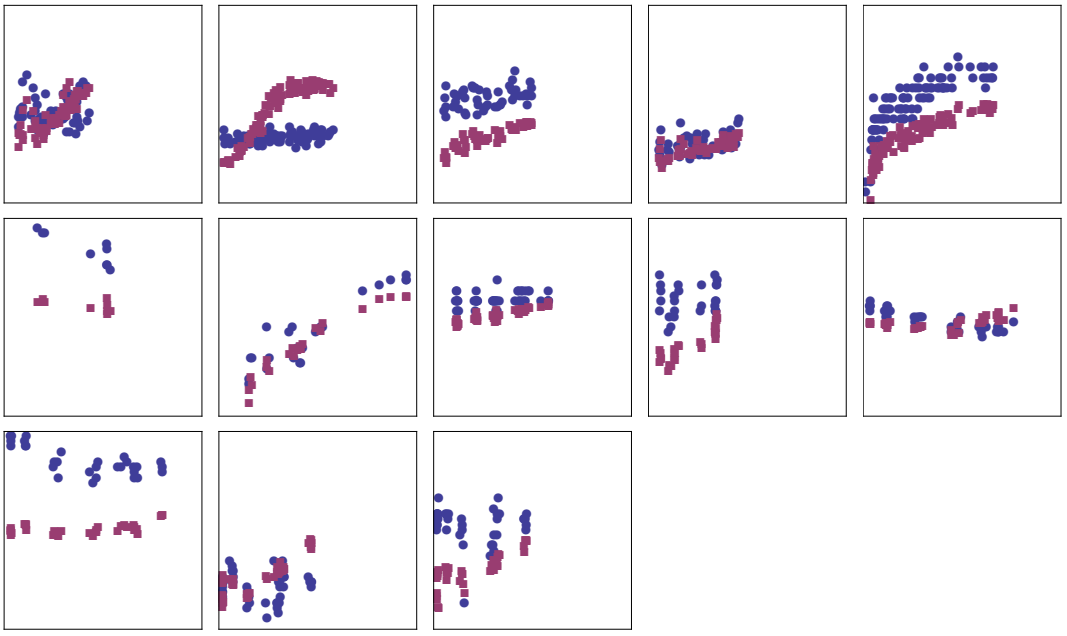

Figure 29: τ_i (blue) and τ_f (red) as a function of N_p for all measurements. Horiz. scale: $0-19\times10^{10}$, vert. scale 1.0 ns$-$2.9 ns. Measurement No. 1 (top left) to No. 13 (bottom right).

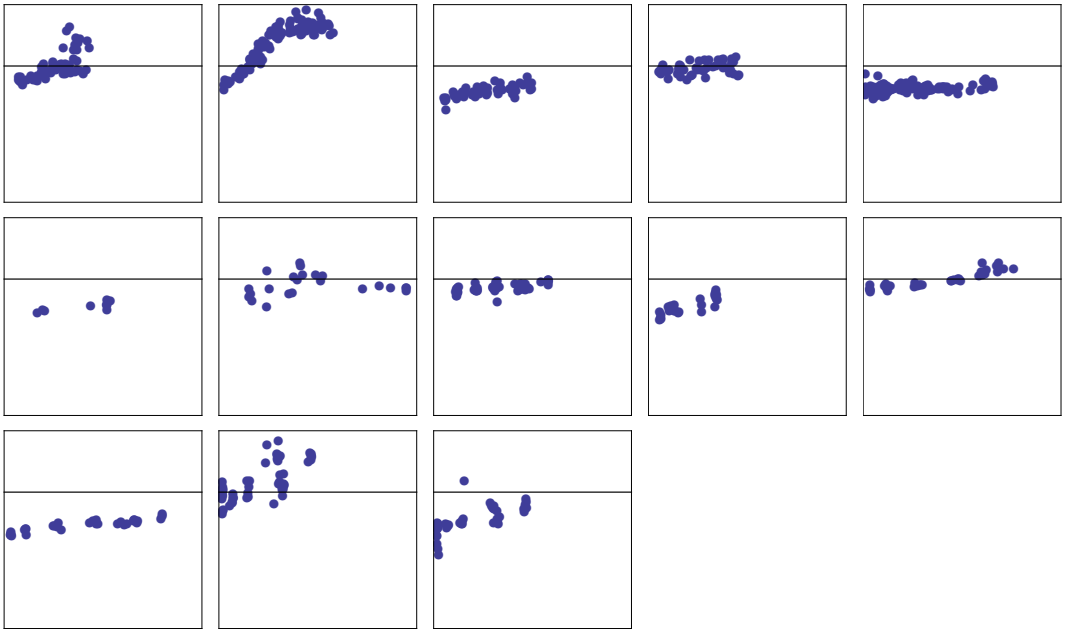

Figure 30: Ratio τ_f/τ_i versus N_p for all measurements. Horiz. scale: $0 - 19 \times 10^{10}$, vert. scale: $0 - 1.45$, horizontal line indicating a ratio of 1. Meas. No. 1 (top left) to No. 13 (bottom right).

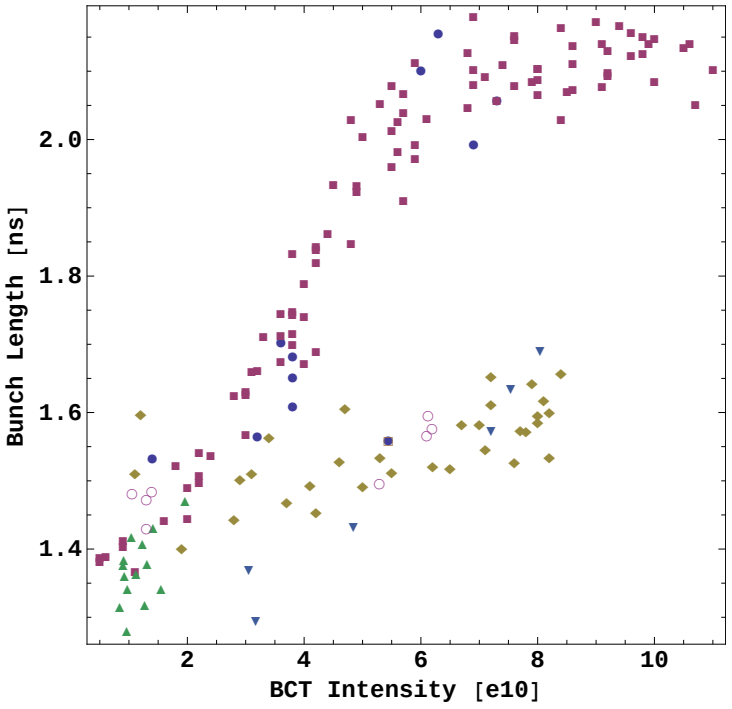

Figure 31: τ_f versus N_p. All measurements, initial bunch length selection 1.5 ns $\leq \tau_i \leq 1.72$ ns. Measurement No. 1 (full blue circle), No. 2 (full red square), no data from No. 3, No. 4 (full yellow diamond), No. 5 (full green triangle), no data from No. 6, No. 7 (full blue triangle), no data from No. 8, No. 9, No. 10, No. 11, No. 12 (empty red circle), No. 13 (empty yellow square).

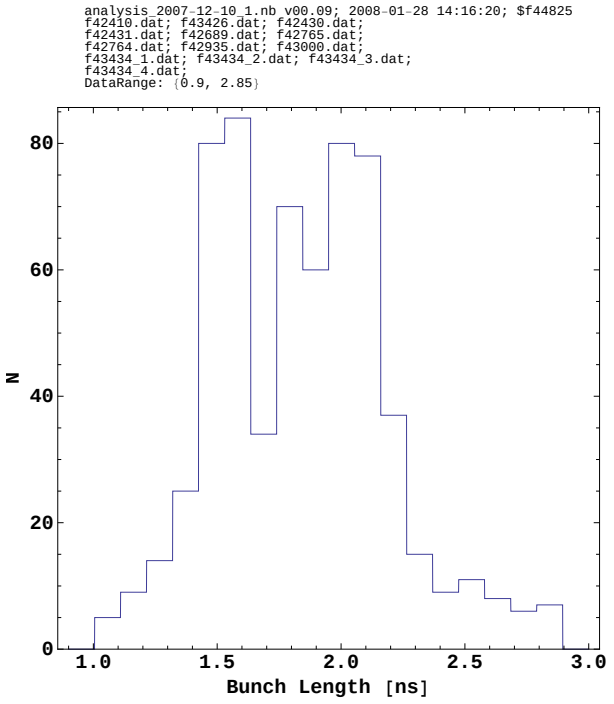

Figure 32: Distribution of τ_i of all measurements.

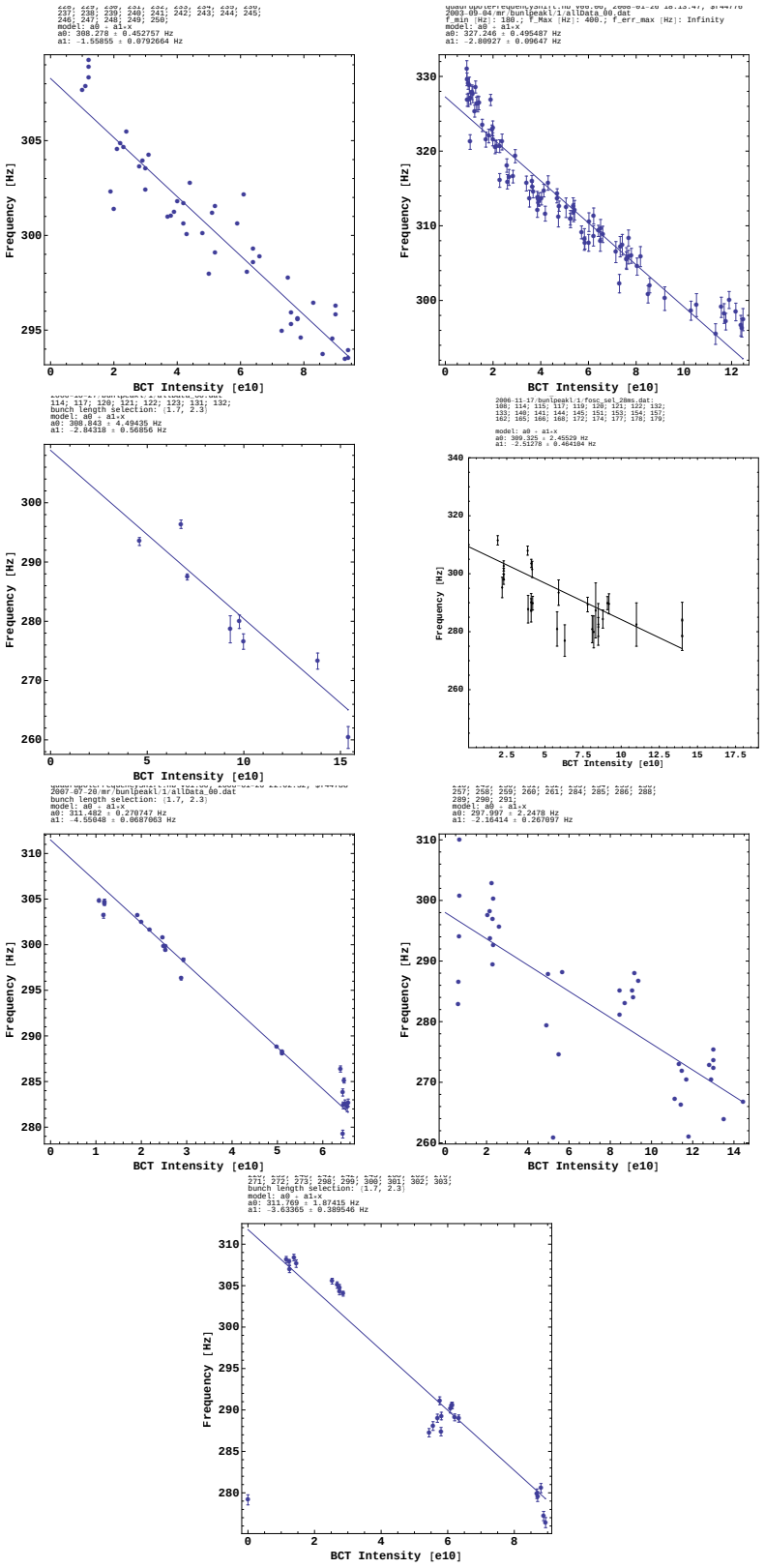

Figure 33: Quadrupole oscillation frequency at injection versus N_p for Measurement No. 3 (top left), No. 5, No. 7 to No. 10 and No. 13 (bottom) and for data selected according to 1.7 ns$\leq \tau_i \leq$2.3 ns. For the fit results see Table 4 (p. 7).

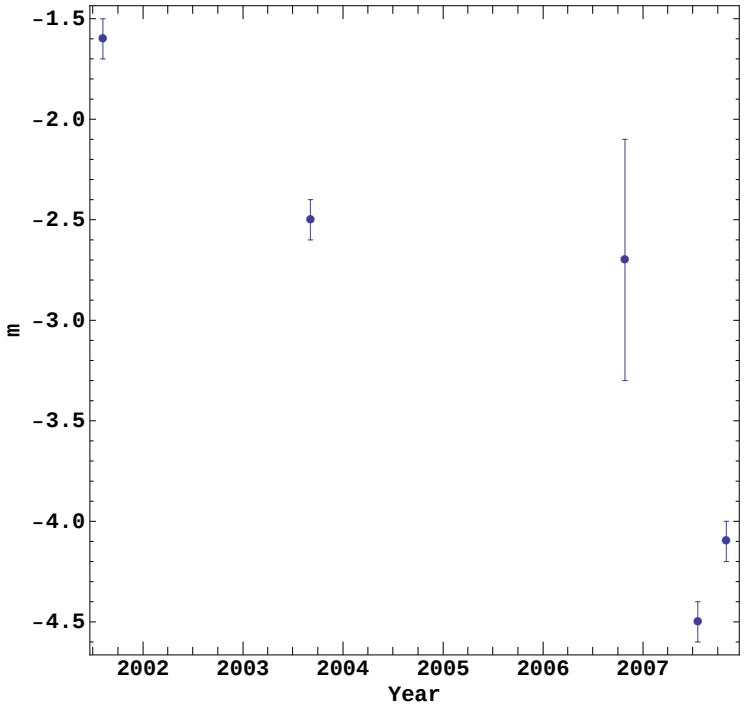

Figure 34: Quadrupole frequency shift versus time for all measurements listed in Table 5 and $0.55 \leq r_{\tau,0} \leq 0.80$. m in units of Hz/10^{10}.

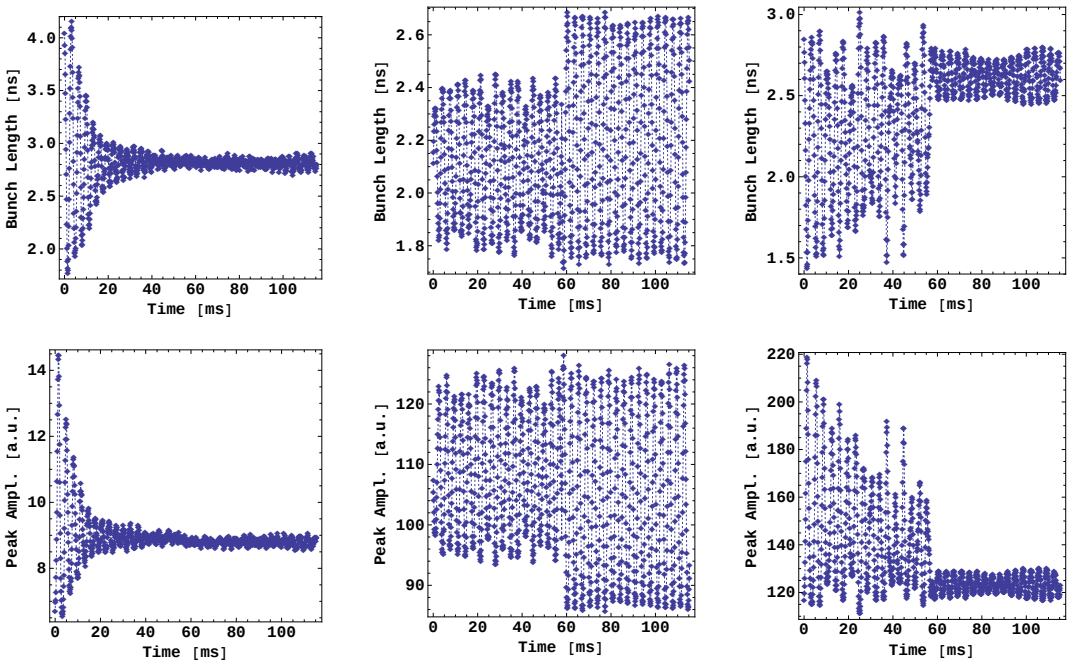

Figure 35: Typical bunch length (4σ, obtained from a Gaussian fit of pick-up and cable transfer function corrected data) and peak amplitude signals for increasing bunch intensity (left to right). The data acquired at injection last from $t = 0$ to about $t = 60$ ms, the data acquired at 600 ms start at about $t = 60$ ms in this plot. Data of 2007-11-01.

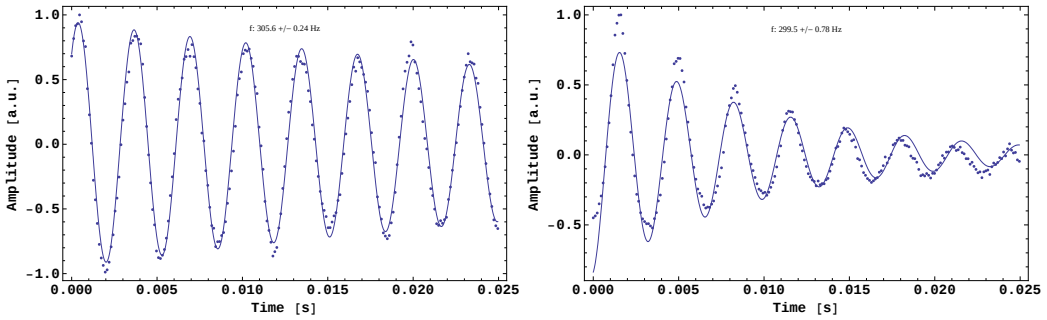

Figure 36: Typical quadrupole oscillation at injection for two cases. Data of 2007-11-01.

References

[1] Shaposhnikova, E., *Present knowledge of the longitudinal SPS impedance*, 10th Workshop on LEP-SPS Performance, Chamonix, France, 17 - 21 January 2000, pp. 72-77.

[2] Shaposhnikova, E., *Impedance measurements*, SPS Studies Working Group, Ed. F. Zimmermann, Minutes of 2001-08-21.

[3] Bohl, T., T. Linnecar, E. Shaposhnikova, *Effect of the SPS impedance reduction on longitudinal bunch stability*, SL-Note-2001-040 MD, CERN, Geneva, October 2001.

[4] Bohl, T., T. Linnecar, E. Shaposhnikova, *Impedance reduction in the CERN SPS as seen from longitudinal beam measurements*, Proc. EPAC 2002, Paris, France.

[5] Shaposhnikova, E., *Impedance effects in the SPS*, Proc. 1st LHC Project Workshop, Chamonix, France, 19 - 23 Jan 2004, pp. 44-50

[6] Bohl, T., Linnecar, T., Shaposhnikova, E., Tueckmantel, J., *Measurement of quadrupole frequency shift below transition*, AB Note 2004-047 MD, CERN, Geneva, May 2004.

[7] Tueckmantel, J. et al., *SPS longitudinal impedance measurements*, Presentation at CERN AB Department Accelerator Physics Committee (APC), 2006-11-10.

[8] Shaposhnikova, E., *Measurement of the low frequency part of the SPS longitudinal impedance: preliminary results*, Presentation at CERN AB Department Accelerator Physics Committee (APC), 2007-08-03.

[9] Shaposhnikova, E., *Measurement of the low frequency part of the SPS longitudinal impedance: second attempt*. Presentation at CERN AB-RF-BR Section Meeting, 2007-11-13, private communication.

[10] Comblin, J.-F., S. Hancock, J.-L. Sanchez Alvarez, *A pedestrian guide to online phase space tomography in the CERN PS complex*. PS/RF/Note 2001-10 Revised. Geneva, November 2004.

[11] Linnecar, T., *The high frequency longitudinal and transverse pick-ups used in the SPS*, SPS ARF 78-17, CERN, Geneva, August 1978.

[12] Bohl, T., *Bunch length measurements with the SPS AEW.31731 wall current monitor*, AB Note 2007-32 (RF), CERN, Geneva, June 2007.

[13] Sanchez Alvarez, J.-L., *PS bunch shape measurement.* PS/OP/Note 98-09 (Tech.), Geneva, February 1998.